Vibrational Analysis of Vacuum Ultraviolet Mass-Analyzed Threshold Ionization Spectra of Phenylacetylene and Benzonitrile

Chan Ho Kwon, Hong Lae Kim,[†] and Myung Soo Kim*

National Creative Research Initiative Center for Control of Reaction Dynamics and School of Chemistry, Seoul National University, Seoul 151-742, Korea

One-photon MATI spectra of phenylacetylene and benzonitrile were obtained by using vacuum ultraviolet radiation generated by four-wave difference frequency mixing in Kr. Accurate ionization energies of phenylacetylene and benzonitrile were determined from the positions of the 0−0 bands, which are 8.8195 ± 0.0006 and 9.7288 ± 0.0006 eV, respectively. Vibrational frequencies of the molecular ions were determined from the spectra also. Assignments were made by utilizing the symmetry selection rule and frequencies and Franck−Condon factors calculated at the BP86, B3LYP, and B3PW91 density functional theory levels with the 6-311++G(2df,2pd) basis set.

I. Introduction

Structure, thermochemical properties, and dynamics of ions are of fundamental interest in relation to studies of combustion, atmospheric chemistry, cosmochemistry, etc.[1−3] Information on ionic vibrational structures is especially useful to probe ions in complex mixtures or follow complicated reaction processes. Nowadays, conventional spectroscopic techniques such as high-resolution photoelectron or laser-induced fluorescence spectroscopies have been popular in characterizing polyatomic ions.[4,5] However, obtaining vibrational spectra of polyatomic ions with these techniques is a formidable job because of their limited capabilities. The resolution of photoelectron spectroscopy (PES), which is typically 10 meV (80 cm^{-1}), is not good enough to obtain vibrational information on polyatomic cations, even though PES is useful to investigate electronic states.[6] The laser-induced fluorescence spectroscopy, which usually has higher resolution than PES and can resolve vibrational peaks, is not generally applicable because most of the excited electronic states of polyatomic cations do not fluoresce.[7]

Zero kinetic energy (ZEKE) photoelectron spectroscopy has a much better resolution than ordinary PES and hence can obtain even rotational information for simple molecular ions.[8−10] Mass-analyzed threshold ionization (MATI) basically employs the same principle as ZEKE except for detecting ions instead of electrons and hence providing mass-selectivity in the spectra.[11−13] Generally adopted in the ZEKE or MATI spectroscopies is a two-color $1 + 1'$ scheme. Namely, excitation to a Rydberg state is achieved in two steps via an intermediate state. However, because the first excited states of most of the molecules are located in the region beyond commercial dye laser outputs (>210 nm) and these states in many cases are either unbound or relax rapidly, use of this scheme suffers the major limitation of low transition probability to the Rydberg state. One-photon ZEKE/MATI using tunable vacuum ultraviolet (VUV) radiation can overcome such difficulties because the transition occurs directly from the ground state to a Rydberg state, not mediated by an excited electronic state of the neutral.[14−17]

One-photon MATI spectra of benzene and halobenzenes reported recently by this laboratory showed well-resolved vibrational peaks of the corresponding cations, which consisted mostly of fundamentals with proper symmetries.[18−21] Vibrational assignments were made by referring to the previous results, comparing with calculated frequencies, and invoking the selection rule for one-photon process. Difference in the geometry between the neutral and cation, or geometric change upon ionization, was calculated quantum chemically and used to explain the prominent overtones of some vibrational modes and combinations involving these. As a more rigorous attempt to utilize spectral intensity information for vibrational assignment, Franck−Condon factors were calculated from the quantum chemical results in our recent study of some aliphatic halides.[22,23] Theoretical prediction of the intensities for transitions to all of the totally symmetric vibrational states was found to be extremely useful for reliable assignment.

In this paper, we report the vibrational spectra of phenylacetylene and benzonitrile cations obtained by one-photon MATI spectroscopy. Successful vibrational assignments made on the basis of the above strategy, namely, by utilizing the calculated frequencies and Franck−Condon factors and symmetry selection rule, will be presented also.

II. Experimental Section

Phenylacetylene and benzonitrile were purchased from Aldrich and Kanto, respectively, and used without further purification. A gaseous sample seeded in He at the stagnation pressure of ~2 atm was supersonically expanded through a temperature-controlled pulsed nozzle (diam 500 μm, General Valve) and introduced to an ionization chamber through a skimmer (diam 2 mm, Beam Dynamics) placed about 3 cm downstream from the nozzle orifice. The background pressure in the ionization chamber was typically ~10^{-8} Torr.

The experimental setup was described in detail previously.[18,19] Briefly, to excite the Kr 5p[$^1/_2$]$_0$−4p^6 transition for VUV generation by four wave difference frequency mixing, the light at 212.5 nm (~0.5 mJ/pulse) was generated by frequency tripling

---

* To whom correspondence should be addressed. E-mail: myungsoo@plaza.snu.ac.kr. Tel: +82-2-880-6652. Fax: +82-2889-1568.
† Permanent address: Department of Chemistry, Kangwon National University, Chuncheon 200-701, Korea.

TABLE 1: Vibrational Frequencies (in cm^{-1}) of Phenylacetylene Neutral and Cation in the Ground Electronic States Calculated at the B3LYP, B3PW91, and BP86 Levels with the 6-311++G(2df,2pd) Basis Set and Experimental Data for the Neutral

mode	symm	neutral				cation		
		expt[a]	B3LYP	B3PW91	BP86	B3LYP	B3PW91	BP86
1	a$_1$	763	777	781	756	766	767	746
2	a$_1$	3064	3202	3210	3125	3221	3228	3144
3	b$_2$	1283	1310	1325	1290	1298	1304	1257
4	b$_1$	691	708	707	683	741	738	699
5	b$_1$	986	1014	1011	968	1045	1040	999
6a	a$_1$	467	474	471	459	470	467	455
6b	b$_2$	619	638	648	616	581	578	560
7a	a$_1$	3035	3172	3179	3094	3196	3201	3119
7b	b$_2$		3198	3206	3121	3219	3226	3142
8a	a$_1$	1598	1640	1651	1587	1643	1652	1592
8b	b$_2$	1573	1609	1621	1558	1536	1538	1483
9a	a$_1$	1178	1202	1198	1163	1210	1206	1172
9b	b$_2$	1158	1185	1180	1149	1175	1174	1139
10a	a$_2$	842	860	859	825	827	824	789
10b	b$_1$	165	142	142	136	120	118	115
11	b$_1$	756	782	777	752	817	815	787
12	a$_1$	1000	1018	1017	987	998	999	971
13	a$_1$	1192	1223	1228	1193	1266	1271	1228
14	b$_2$	1331	1358	1357	1325	1387	1393	1348
15	b$_2$		161	159	152	153	151	145
16a	a$_2$	418	413	409	395	363	358	345
16b	b$_1$	531	558	558	536	481	479	457
17a	a$_2$	971	998	996	953	1027	1024	982
17b	b$_1$	918	946	944	904	991	988	949
18a	a$_1$	1028	1050	1053	1020	1009	1011	981
18b	b$_2$	1071	1102	1103	1069	1113	1115	1081
19a	a$_1$	1489	1526	1525	1474	1486	1483	1435
19b	b$_2$	1444	1478	1477	1429	1436	1442	1399
20a	a$_1$	3083	3191	3198	3113	3210	3216	3133
20b	b$_2$	3058	3180	3188	3103	3208	3214	3130
βCC	b$_2$	516	539	538	517	531	528	507
βCH	b$_2$	653	689	690	635	694	695	645
νCC	a$_1$	2118	2202	2209	2131	2107	2108	2053
νCH	a$_1$	3291	3468	3472	3393	3409	3412	3334
γCC	b$_1$	352	371	369	354	324	322	311
γCH	b$_1$	610	645	633	588	645	642	621

[a] Reference 33.

TABLE 2: Vibrational Frequencies (in cm^{-1}) of Benzonitrile Neutral and Cation in the Ground Electronic States Calculated at the B3LYP, B3PW91, and BP86 Levels with the 6-311++G(2df,2pd) Basis Set and Experimental Data for the Neutral

mode	symm	neutral				cation		
		expt[a]	B3LYP	B3PW91	BP86	B3LYP	B3PW91	BP86
1	a$_1$	769	774	774	752	755	756	736
2	a$_1$	3071	3196	3215	3130	3210	3228	3143
3	b$_2$	1289	1319	1334	1298	1416	1426	1382
4	b$_1$	686	706	704	682	631	628	607
5	b$_1$	987	1021	1016	974	1042	1035	994
6a	a$_1$	461	467	465	452	459	456	445
6b	b$_2$	629	641	637	619	504	500	483
7a	a$_1$	3042	3178	3185	3100	3196	3201	3118
7b	b$_2$	3027	3204	3212	3127	3219	3225	3141
8a	a$_1$	1599	1641	1654	1588	1660	1669	1603
8b	b$_2$	1584	1615	1627	1563	1275	1279	1235
9a	a$_1$	1178	1203	1200	1165	1210	1207	1172
9b	b$_2$	1163	1188	1184	1153	1148	1150	1110
10a	a$_2$	848	863	862	828	814	811	775
10b	b$_1$	172	147	146	140	118	116	111
11	b$_1$	758	781	780	751	815	813	784
12	a$_1$	1001	1019	1019	989	1001	1000	971
13	a$_1$	1191	1220	1226	1188	1252	1256	1215
14	b$_2$	1337	1361	1361	1329	1392	1389	1344
15	b$_2$	162	169	166	160	157	155	148
16a	a$_2$	401	410	406	392	353	347	335
16b	b$_1$	548	573	574	552	449	442	413
17a	a$_2$	978	1002	1000	957	1029	1025	983
17b	b$_1$	925	954	952	912	990	985	947
18a	a$_1$	1027	1050	1053	1021	984	988	962
18b	b$_2$	1071	1105	1106	1073	1088	1093	1054
19a	a$_1$	1492	1528	1527	1475	1474	1469	1425
19b	b$_2$	1448	1480	1480	1431	1528	1529	1475
20a	a$_1$	3080	3207	3203	3118	3221	3216	3132
20b	b$_2$	3039	3188	3195	3110	3209	3214	3131
βCN	b$_2$	551	570	570	549	568	570	548
νCN	a$_1$	2232	2332	2341	2236	2192	2196	2124
γCN	b$_1$	381	392	390	375	317	312	298

[a] Reference 33.

[a] Reference 33.

of 637.6 nm output of a dye laser (Continuum ND6000) pumped by the second harmonic of an Nd:YAG laser (Continuum PL8000). Another dye laser output (430−760 nm) pumped by the second or third harmonic of the second Nd:YAG laser (Continuum Surelite II) was combined with the 212.5 nm light and loosely focused with a fused silica lens (f = 50 cm) in the Kr cell to generate the VUV light tunable in the 123−141 nm region. A MgF$_2$ lens (f = 25 cm) was placed at the exit of the Kr cell, and the laser beams were aligned off-centered at the lens to separate the residual light beams (UV and visible) from the VUV light, which was focused onto the molecular beam. The optimized Kr pressure in the cell was 5−18 Torr. Small portions of dye laser outputs were used to calibrate their frequencies on the basis of the optogalvanic effect in an Fe/Ne hollow cathode lamp.[24] Its precision was ±0.5 cm^{-1} in the visible region.

The VUV laser pulse was collinearly overlapped with the molecular beam in a counter-propagation manner and slit-electrodes along the beam path were used to maximize ion collection efficiency. The spoil field of 0−0.2 V/cm was applied in the ionization region to remove directly produced ions. To achieve pulsed-field ionization (PFI) of neutrals in the ZEKE state, an electric field of 15−60 V/cm was applied at a certain delay time after the laser pulse. Ions were then accelerated, flew through a field-free region, and were detected by a dual microchannel plate detector. A short pulse of the scrambling field was applied at the laser irradiation time, which significantly lengthened the lifetime of the ZEKE states. Use of a long delay time ($\sim$20 μs) and low spoil field tremendously improved the quality of the MATI spectra. A gold wire was placed in the VUV beam path as a beam monitor.[25] Its output was used to normalize the intensity of each vibrational peak in the MATI spectra.

III. Vibrational Analysis

A. Quantum Chemical Calculations. Calculations of equilibrium geometries and vibrational frequencies of phenylacetylene and benzonitrile and their cations in the ground states were performed at the density functional theory (DFT) levels, B3LYP, B3PW91, and BP86, with various basis sets using Gaussian 98 suite of programs.[26] Size of the basis set was systematically increased until the basis set dependence disappeared. Hence, only those obtained with the largest basis set used, the 6-311++G(2df,2pd), will be listed and discussed. For the vibrational frequencies, the results obtained at the BP86/6-311++G(2df,2pd) level showed the best agreement with the experimental data. Frequencies obtained by these calculations are presented without scaling in Tables 1 and 2.

B. Symmetry Selection Rules. In our previous investigation of one-photon MATI spectra of benzene,[20] symmetry selection rules for transitions from the ground-state neutral to Rydberg states were extremely helpful for the vibrational peak assignments. The selection rules pertinent to the present systems are summarized as follows.
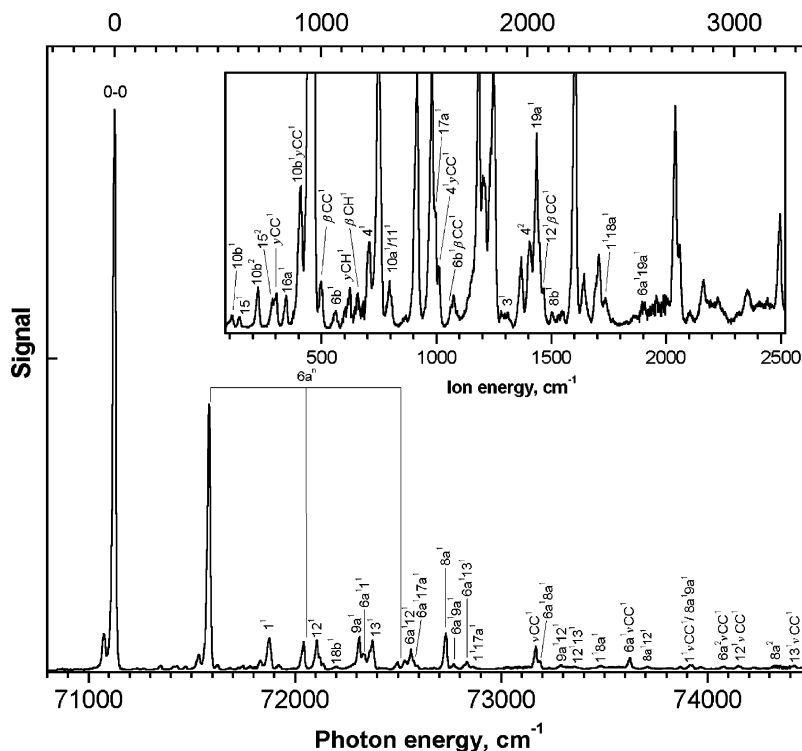
Figure 1. One-photon MATI spectrum of $C_6H_5C{\equiv}CH$ recorded by monitoring $C_6H_5C{\equiv}CH^+$ in the ground electronic state. The *x*-scale at the top of the figure corresponds to the vibrational frequency scale for the cation the origin of which is at the 0−0 band position. Spectrum in the 50−2500 cm^{-1} region magnified by 15 is shown as an inset to demonstrate the quality of the MATI spectrum obtained in this work.

Under the Born−Oppenheimer approximation, the transition moment for Rydberg (R) ← ground (G) vibronic transition can be expressed as the product of the electronic (e) and vibrational (v) parts. Upon further approximation of the electronic wave function of a Rydberg state as the product of the electronic wave function of the ion core (Ψ_e^C) and that of the Rydberg electron (Ψ_e^R), these become $\langle\Psi_e^G|\bar{\mu}|\Psi_e^C\Psi_e^R\rangle$ and $\langle\Psi_v^G|\Psi_v^C\rangle$, respectively. For a high Rydberg state, Ψ_e^C and Ψ_v^C can be approximated as those of the corresponding ionic state. Detailed analysis shows that one can always choose a Rydberg orbital that makes the electronic part allowed. Most of the molecules prepared under the supersonic jet condition are in the zero-point vibrational level, which is totally symmetric, a_1. Hence, in an electric dipole-allowed transition, Ψ_v^C should also belong to a_1. Then, fundamentals and all of the overtones of a_1 modes are allowed, while the $\Delta v = 2, 4, 6, ...$ selection rule holds for nontotally symmetric modes. Also, all of the transitions to the combination states with a_1 symmetry are allowed. Then, the relative intensity of a transition to an a_1 vibrational state, either fundamental, overtone, or combination, is determined by the Franck−Condon factor.[27,28] The methods to evaluate the Franck−Condon factors from quantum chemical results are well established.[22]

IV. Results and Discussion

MATI spectra of phenylacetylene and benzonitrile recorded by monitoring $C_6H_5C{\equiv}CH^+$ and $C_6H_5C{\equiv}N^+$ in the ground electronic states are shown in Figures 1 and 2, respectively. The spectra magnified by 15 are also shown as insets in the figures. The intense peaks appearing at the lowest photon energy, namely, at 71 127 and 78 461 cm^{-1} in Figures 1 and 2, respectively, correspond to the 0−0 bands. The position of the 0−0 band in a one-photon VUV MATI spectrum is equivalent to the ionization energy of the molecule. However, the ionization energy thus measured is usually a little smaller than the correct value because the molecules in ZEKE states[10] some cm^{-1} below

the threshold can also be ionized when a high PFI field is applied. To correct for this effect, the 0−0 band position was measured using various PFI fields, and the accurate ionization energy was estimated by extrapolation to the zero-field limit. Spoil field was not used in such measurements. The ionization energies to the ground electronic states of phenylacetylene and benzonitrile cations measured in this work are listed in Table 3, together with previous results.[29−32] There has been no previous report on the accurate ionization energy of phenylacetylene measured by ZEKE or MATI. The ionization energy of phenylacetylene determined in this work, 8.8195 ± 0.0006 eV, is a little different from 8.825 ± 0.001 eV measured by threshold photoelectron spectroscopy (TPES).[29] More annoying is that the ionization energy of benzonitrile obtained in this work, 9.7288 ± 0.0006 eV, is smaller than a previous ZEKE result[31] by ∼20 cm^{-1}. Our experience is that the present MATI technique, which uses high-voltage electronics, tends to underestimate ionization energies by 0−5 cm^{-1}.[19,20] We do not have an explanation for the above discrepancy at the moment even though we would like to point out that quality of the present MATI spectrum is superior to the previous ZEKE spectrum.[31]

Assuming that the shift of a vibrational peak in a MATI spectrum due to the applied electric fields is similar to that of the 0−0 band, the vibrational frequency corresponding to each peak can be determined simply by taking the difference of its position from that of the 0−0 band. Vibrational frequency scales with origins at the 0−0 band positions are also drawn in Figures 1 and 2. Vibrational frequencies of $C_6H_5C{\equiv}CH^+$ and $C_6H_5C{\equiv}N^+$ in the ground electronic state calculated at the BP86/6-311++G(2df,2pd) level are compared with the experimental data in Tables 4 and 5, respectively. Also listed in the tables are intensities of each peak in the MATI spectra normalized to that of the 0−0 band. Frequencies of some vibrations measured previously by TPES[29] and ZEKE[31] are also included in the tables.

Figure 2. One-photon MATI spectrum of $C_6H_5C\equiv N$ recorded by monitoring $C_6H_5C\equiv N^+$ in the ground electronic state. The *x*-scale at the top of the figure corresponds to the vibrational frequency scale for the cation the origin of which is at the $0-0$ band position. Spectrum in the $50-2200$ cm^{-1} region magnified by 15 is shown as an inset to demonstrate the quality of the MATI spectrum obtained in this work.

TABLE 3: Ionization Energies (IE) of Phenylacetylene and Benzonitrile in eV

	IE ($\tilde{X}$)	ref
phenylacetylene	8.8195 ± 0.0006	this work
	8.825 ± 0.001	TPES[29]
	8.82 ± 0.02	PES[30]
benzonitrile	9.7288 ± 0.0006	this work
	9.7315 ± 0.0002	ZEKE[31]
	9.71 ± 0.01	PI[32]

At all of the levels used in the calculation, equilibrium geometries of the phenylacetylene and benzonitrile neutrals and cations belong to the C_{2v} symmetry. If the symmetry selection rule is invoked, prominent peaks in the MATI spectra must be mostly due to transitions to the a_1 vibrational states. The Franck–Condon factors for such transitions, either fundamentals, overtones, or combinations, calculated at three density functional theory (DFT) levels, B3LYP, B3PW91, and BP86, using the 6-311++G(2df,2pd) basis set were rather similar. The Franck–Condon factors calculated at the BP86/6-311++G(2df,2pd) level and normalized to that of the $0-0$ transition are listed in Tables 4 and 5 also. Comparing the experimental and calculated frequencies and Franck–Condon factors was helpful to identify a_1 peaks. The remaining weak peaks in one-photon MATI spectra must be due to electric dipole-forbidden but vibronically allowed transitions. Only the calculated frequencies, not intensities, can be used to assign these non-totally symmetric transitions.

A. Phenylacetylene. The phenylacetylene cation with C_{2v} symmetry has 36 nondegenerate normal modes,[33] 13 of which belong to the a_1 symmetry species, 3 to a_2, 8 to b_1, and 12 to b_2. Among the a_1-type modes, 2, 7a, 20a, and νCH in Wilson notation[34] are due to CH stretching and have frequencies of $\sim$3000 cm^{-1}. According to our previous study on the CH stretching modes,[22] they are not expected to appear distinctly in the one-photon MATI spectrum. Then, prominent peaks in

the spectral region $0-1700$ cm^{-1} and near $\sim$2000 cm^{-1} can mostly be assigned to the fundamentals of the remaining a_1 modes, 1, 6a, 8a, 9a, 12, 13, 18a, 19a, and νCC, as well as their overtones and combinations. Among these, the calculated Franck–Condon factors are especially significant for the fundamentals of 6a, 1, 12, 9a, 8a, and νCC of which the calculated frequencies at the BP86 level are 455, 746, 971, 1172, 1592, and 2053 cm^{-1}, respectively. Hence, the prominent peaks at 458, 747, 979, 1185, 1604, and 2040 cm^{-1} in the MATI spectrum of phenylacetylene can readily be assigned to $6a^1$, 1^1, 12^1, $9a^1$, $8a^1$, and νCC^1, respectively. Even though the fundamental of ν_{13}, which is another a_1-type mode, is expected to be weak according to its calculated Franck–Condon factor, it appears distinctly near its calculated frequency at 1249 cm^{-1}. $19a^1$ appears rather distinctly at 1435 cm^{-1}, even though its calculated Franck–Condon is only 0.004. We would rather assign this to a composite of $19a^1$ and $6a^1 12^1$ on the basis of the calculated frequencies and Franck–Condon factors. A weak shoulder peak at 989 cm^{-1} is close to 981 cm^{-1} calculated for $18a^1$. We are reluctant to make such an assignment because the calculated Franck–Condon factor for this transition is extremely small, 0.0002. It is to be mentioned that the harmonic frequencies calculated at the BP86 level are usually a little smaller than the experimental ones, while those at the B3LYP and B3PW91 levels are larger. The same trend holds for most of the fundamentals of the phenylacetylene and benzonitrile neutrals as can be seen in Tables 1 and 2. Even though the results must rise from different error cancellations at these levels,[35] the correlation can be used advantageously in the peak assignments.

The fact that $6a^1$ appeared most prominently in the one-photon MATI spectrum indicates that the geometrical change upon ionization occurs mostly along the 6a eigenvector. This was confirmed by calculation, even though not shown here, by projecting the geometrical change vector on the 6a eigenvector. This also suggests that $6a^n$ overtones and combinations of 6a

Vibrational Analysis of VUV-MATI Spectra

J. Phys. Chem. A, Vol. 107, No. 50, 2003 **10973**

TABLE 4: Vibrational Frequencies (in cm^{-1}) and Their Assignments for Phenylacetylene Cation in the Ground Electronic State ($\tilde{X}^2B_1$)

mode[a]	symm	TPES[b]	calculated[c] freq	calculated[c] intensity[d]	this work freq	this work intensity[d]	mode[a]	symm	TPES[b]	calculated[c] freq	calculated[c] intensity[d]	this work freq	this work intensity[d]
							Fundamentals						
1	a$_1$	759	746	0.131	747	0.076	14	b$_2$		1348	0		
2	a$_1$		3144	5 × 10^{-6}			15	b$_2$		145	0	143	0.005
3	b$_2$		1257	0	1287	0.007	16a	a$_2$		345	0	346	0.011
4	b$_1$		699	0	706	0.017	16b	b$_1$		457	0		
5	b$_1$		999	0	996	0.008	17a	a$_2$		982	0	989	0.006
6a	a$_1$	460	455	0.353	458	0.438	17b	b$_1$		949	0		
6b	b$_2$		560	0	561	0.008	18a	a$_1$		981	0.0002		
7a	a$_1$		3119	3 × 10^{-6}			18b	b$_2$		1081	0	1076	0.007
7b	b$_2$		3142	0			19a	a$_1$		1435	0.004	1435[f]	0.044
8a	a$_1$		1592	0.096	1604	0.073	19b	b$_2$		1399	0		
8b	b$_2$		1483	0	1505	0.006	20a	a$_1$		3133	0.0003		
9a	a$_1$		1172	0.081	1185	0.102	20b	b$_2$		3130	0		
9b	b$_2$		1139	0	1158	0.018	βCC	b$_2$	504	507	0	499	0.012
10a	a$_2$		789	0	795[e]	0.015	βCH	b$_2$		645	0	658	0.008
10b	b$_1$		115	0	110	0.008	νCC	a$_1$		2053	0.101	2040	0.042
11	b$_1$		787	0	795[e]	0.015	νCH	a$_1$		3334	0.0001		
12	a$_1$		971	0.069	979	0.066	γCC	b$_1$		311	0	303	0.010
13	a$_1$		1228	0.010	1249	0.087	γCH	b$_1$		621	0	622	0.010
							Overtones and Combinations						
10b^2	a$_1$		230	0.002	221	0.010	6a^{1}19a^1	a$_1$		1890	0.002	1895	0.017
15^2	a$_1$		290	0.0002	286	0.007	6a^{1}8a^1	a$_1$		2047	0.035	2058	0.017
10b^{1}γCC^1	a$_1$		426	0.002	409	0.034	9a^{1}12^1	a$_1$		2143	0.005	2164	0.017
6a^{1}10b^{1}γCC^1	a$_1$		881	0.0007	865	0.006	12^{1}13^1	a$_1$		2199	0.001	2228	0.013
6a^2	a$_1$		910	0.065	914	0.063	1^{1}8a^1	a$_1$		2338	0.011	2356	0.016
4^{1}γCC^1	a$_1$		1010	0.0003	1009	0.012	6a^{1}νCC^1	a$_1$		2508	0.038	2496	0.027
6b^{1}βCC^1	a$_1$		1067	0.0004	1064	0.005	8a^{1}12^1	a$_1$		2563	0.005	2582	0.012
6a^{1}1^1	a$_1$		1201	0.045	1205	0.082	1^{1}νCC^1	a$_1$		2764	0.008	2789	0.016
6a^3	a$_1$		1365	0.008	1370	0.022	8a^{1}9a^1	a$_1$		2799	0.012		
4^2	a$_1$		1398	0.008	1407	0.028	19a^{1}19b^1	b$_2$		2834	0	2837	0.007
6a^{1}12^1	a$_1$		1426	0.026	1435[f]	0.044	6a^{2}νCC^1	a$_1$		2963	0.007	2953	0.011
6a^{1}17a^1	a$_2$		1437	0	1448	0.009	12^{1}νCC^1	a$_1$		3024	0.008	3022	0.010
12^{1}βCC^1	b$_2$		1478	0	1465	0.007	6a^{1}8a^{1}12^1	a$_1$		3018	0.002	3032	0.008
6a^{1}9a^1	a$_1$		1627	0.029	1643	0.017	8a^2	a$_1$		3184	0.006	3206	0.014
6a^{1}13^1	a$_1$		1683	0.004	1706	0.025	9a^{1}νCC^1	a$_1$		3224	0.010	3227	0.011
1^{1}17a^1	a$_2$		1728	0	1739	0.010	13^{1}νCC^1	a$_1$		3281	0.002	3292	0.010

^{a} Wilson notation. ^{b} Reference 29. ^{c} BP86/6-311++G(2df,2pd) level. ^{d} Normalized to the intensity of the 0−0 band. ^{e} A composite of 10a^1 and 11^1. ^{f} A composite of 19a^1 and 6a^{1}12^1.

and other a$_1$ modes would appear prominently in the one-photon MATI spectrum. Accordingly, the prominent peaks at 914 and 1370 cm^{-1} can be assigned to 6a^2 and 6a^3, respectively. Also, the distinct peaks at 1205, 1435, 1643, 1706, 2058, and 2496 can be assigned to 6a combinations, 6a^{1}1^1, 6a^{1}12^1, 6a^{1}9a^1, 6a^{1}13^1, 6a^{1}8a^1, and 6a^{1}νCC^1, respectively, from the calculated frequencies and Franck−Condon factors. The peak at 1435 cm^{-1} can be alternatively assigned to 19a^1 as has been mentioned earlier. Other combinations of the a$_1$ modes, 1^{1}18a^1, 9a^{1}12^1, and 1^{1}8a^1, appeared distinctly also at 1739, 2164, and 2356 cm^{-1}, respectively. The Franck−Condon factors for 1^{1}νCC^1 and 8a^1-9a^1 calculated at the BP86 level are 0.012 and 0.008, respectively. Hence, the peak at 2789 cm^{-1}, which can be assigned either to 1^{1}νCC^1 or to 8a^{1}9a^1 on the basis of the frequencies may better be assigned to a composite of the two transitions, 1^{1}νCC^1/8a^{1}9a^1. The calculated Franck−Condon factors for the fundamentals of the CH stretching modes 2, 7a, 20a, and νCH are negligible. This is understandable because the lengths of all of the CH bonds hardly change upon ionization. Extremely weak peaks appeared in the 3000−3200 cm^{-1} region of the present MATI spectrum (Figure 1). We are reluctant to assign them to 2^1, 7a^1, 20a^1, or νCH^1 because their calculated Franck−Condon factors are very small. Instead, it is more likely that they are overtones or combinations. Thus, the very weak peaks at 3022, 3206, and 3292 were assigned to 12^{1}νCC^1, 8a^2, and 13^{1}νCC^1, respectively. Some distinct peaks may be assigned to

combinations of nontotally symmetric modes with a$_1$ overall symmetry. Hence, the distinct peaks at 221, 286, 409, 1009, and 1407 were assigned to 10b^2, 15^2, 10b^{1}γCC^1, 4^{1}γCC^1, and 4^2, respectively.

The fundamentals of nontotally symmetric modes are forbidden under the Born−Oppenheimer approximation. They still appeared in the actual spectrum, even though very weakly, through vibronic mechanism. Hence, very weak peaks at 303, 346, 499, 561, 622, 706, and 795 cm^{-1} can be assigned to γCC^1, 16a^1, βCC^1, 6b^1, γCH^1, 4^1, and 10a^1/11^1 by comparing with the calculated frequencies of 311, 345, 507, 560, 621, 699, and 789/787 cm^{-1}, respectively. A very weak 16b^1 is expected at ~457 cm^{-1} but must have been buried in the strong 6a^1 transition. Similarly, 17a^1 and 17b^1 expected at 950−980 cm^{-1} may have been buried as shoulders of 12^1. The weak shoulder peak at 989 cm^{-1} mentioned previously may be 17a^1 rather than 18a^1.

B. Benzonitrile. Kimura and co-workers reported the 1 + 1′ ZEKE spectrum of benzonitrile in the 0−1200 cm^{-1} vibrational energy region.[31] Tentative assignments were made by comparing with results from PM3 semiempirical calculation. They adopted Mulliken notation for vibration modes, with some minor errors. We reinterpreted their assignments using the DFT frequencies calculated in this work and listed them in Table 5.

A spectrum with much better quality than the above was obtained in the 0−2500 cm^{-1} region (78 200−81 000 cm^{-1} in

TABLE 5: Vibrational Frequencies (in cm⁻¹) and Their Assignments for Benzonitrile Cation in the Ground Electronic State ($\tilde{X}^2B_1$)

mode[a]	symm	ZEKE[b]	calculated[c] freq	intensity[d]	this work freq	intensity[d]
			Fundamentals			
1	a_1		736	0.213	737	0.098
2	a_1		3143	0.0001		
3	b_2		1382	0	1386	0.011
4	b_1		607	0	606	0.022
5	b_1	1036	994	0	1034	0.047
6a	a_1	447	445	0.295	438	0.376
6b	b_2	559	483	0		
7a	a_1		3118	2×10^{-7}		
7b	b_2		3141	0		
8a	a_1		1603	0.143	1612	0.032
8b	b_2		1235	0		
9a	a_1		1172	0.098	1168	0.072
9b	b_2		1110	0	1111	0.025
10a	a_2	854	775	0	771[e]	0.017
10b	b_1	110	111	0	111	0.016
11	b_1		784	0	771[e]	0.019
12	a_1		971	0.036	968	0.039
13	a_1		1215	0.001	1223	0.024
14	b_2		1344	0	1353	0.020
15	b_2	144	148	0	143	0.011
16a	a_2	332	335	0	336	0.011
16b	b_1	405	413	0	412	0.022
17a	a_2	1005	983	0	984	0.011
17b	b_1	920	947	0	922[f]	0.025
18a	a_1		962	0.081	959	0.047
18b	b_2		1054	0		
19a	a_1		1425	0.001	1413[g]	0.017
19b	b_2		1475	0	1470[h]	0.011
20a	a_1		3132	1×10^{-5}		
20b	b_2		3131	0		
βCN	b_2	537	548	0	536	0.015
νCN	a_1		2124	0.055	2136	0.037
γCN	b_1		298	0	291	0.018
			Overtones and Combinations			
$10b^2$	a_1	219	222	0.005	223	0.015
$10b^2 15^1$	b_2		370	0	361	0.037
$6a^1 10b^2$	a_1		667	0.002	662	0.011
$4^1 10b^1$	a_1		718	0.001	712	0.022
$16b^2$	a_1		826	0.017	854	0.091
$6a^2$	a_1		890	0.045		
$6b^2$	a_1		966	0.009	922[f]	0.023
4^2	a_1		1214	0.0004	1212	0.015
$6a^1 12^1$	a_1		1416	0.012	1413[g]	0.017
1^2	a_1		1472	0.020	1470[h]	0.011
$6a^1 13^1$	a_1		1660	0.0003	1647	0.008
$1^1 18a^1$	a_1		1698	0.017	1724	0.034
$1^1 12^1$	a_1		1707	0.006		
$1^1 9b^1$	b_2		1846	0	1841	0.011
$1^1 9a^1$	a_1		1908	0.018	1903	0.013
1^3	a_1		2208	0.001	2205	0.036

a Wilson notation. *b* Reference 31. *c* BP86/6-311++G(2df,2pd) level. *d* Normalized to the intensity of the 0–0 band. Intensity of the peaks above 1700 cm⁻¹ is not accurate due to very weak VUV power. *e* A composite of $10a^1$ and 11^1. *f* A composite of $17b^1$ and $6b^2$. *g* A composite of $19a^1$ and $6a^1 12^1$. *h* A composite of $19b^1$ and 1^2.

photon energy) by one-photon MATI in this work. The 81 000–81 500 cm⁻¹ region could not be recorded because of a dip in VUV output. According to our experience in MATI of phenylacetylene in this work and halobenzenes in previous studies,[18,19] this region is not expected to be important because the CH stretching fundamentals would not be observed anyway. Symmetry selection rule and frequencies and Franck–Condon factors calculated at the DFT levels will be utilized to assign the observed vibrational peaks as has been done for phenylacetylene. VUV power above 1700 cm⁻¹ in vibrational energy was very weak. Hence, the calibrated relative intensities of peaks above 1700 cm⁻¹ may be rather inaccurate.

Quantum chemical calculations performed at various levels for this molecule suggest that the cation belongs to the C_{2v} point group in the ground electronic state. Twelve normal modes are a_1-type as listed in Table 2. Among these, 2, 7a, and 20a are high-frequency vibrations with CH stretching character and can be neglected in this work. Among the a_1-type vibrations, the fundamental of 6a displays the largest Franck–Condon factor and is readily identified as the peak at 438 cm⁻¹. Franck–Condon factors are significant for 1^1, $18a^1$, 12^1, $9a^1$, $8a^1$, and νCN^1 with the calculated frequencies of 736, 962, 971, 1172, 1603, and 2124 cm⁻¹, respectively. The prominent peaks at 737, 959, 968, 1168, 1612, and 2136 cm⁻¹ in the MATI spectrum correspond to these transitions. The remaining a_1-type fundamentals are 13^1 and $19a^1$ with the calculated frequencies of 1215 and 1425 cm⁻¹, respectively, and the calculated Franck–Condon factors of only 0.001 for each. Even though one might assign the peak at 1413 cm⁻¹ to $19a^1$ on the basis of the frequency, $6a^1 12^1$ seems to be a better assignment when the intensity is considered also. For 13^1, the peak at 1223 cm⁻¹ is the only candidate even though the calculated and observed intensities show a substantial discrepancy. For the peak at 1223 cm⁻¹, no alternative assignment is possible, to either a fundamental, overtone, or combination. Namely, its assignment to 13^1 is unavoidable, and its small Franck–Condon factor must be attributed to inaccuracy in the calculation. It is to be noted from Table 4 that the Franck–Condon factor for the same transition in phenylacetylene is also much smaller than the experimental intensity, even though not as dramatically as in benzonitrile. It is to be mentioned that Kimura and co-workers did not identify the a_1-type fundamentals, except for $6a^1$, in their 1 + 1' ZEKE work.[31]

Strong fundamental of the 6a mode suggests that its overtones and combinations, especially with other prominent a_1-type modes such as 1, 8a, 9a, 12, 13, 18a, and νCN, would appear distinctly in the one-photon MATI spectrum. $6a^2$ and $6a^3$ overtones are expected to appear at somewhat lower than 876 and 1314 cm⁻¹. Their calculated Franck–Condon factors are 0.045 and 0.005, respectively. They are not easy to identify, however, because of the presence of strong spectral features nearby. The strong peak at 854 cm⁻¹ cannot be matched with the calculated frequency of any fundamental. It may be a composite consisting of $6a^2$ and $16b^2$. We do not attempt to identify $6a^3$ because of its small Franck–Condon factor. The a_1-type combinations involving $6a^1$, namely, $6a^1 12^1$ and $6a^1$-13^1, are identified at 1413 and 1647 cm⁻¹, respectively. The mode 1, which has substantial fundamental intensity, also shows an overtone 1^2 at 1470 cm⁻¹. The a_1-type overtones and combinations involving non-totally symmetric modes are also observed even though with weaker intensities than the a_1 fundamentals. These are $10b^2$, $6a^1 10b^2$, $4^1 10b^1$, and 4^2 at 223, 662, 712, and 1212 cm⁻¹, respectively.

Fundamentals of some non-totally symmetric modes also appear probably through vibronic mechanism. The most noticeable among these are the fundamental, overtone, and combinations of the 10b mode, namely, $10b^1$, $10b^2$, $10b^2 15^1$, $6a^1 10b^2$, and $4^1 10b^1$. $10b^1$ appeared very prominently in the 1 + 1' ZEKE spectrum reported by Kimura and co-workers.[31] It is not as prominent in the present one-photon MATI spectrum. The fact that the initial electronic states involved in the transition moment integral are different in the two processes must be responsible for the above difference. The remaining distinct feature in the MATI spectrum is the peak at 1034 cm⁻¹. Comparing with the

Vibrational Analysis of VUV-MATI Spectra

J. Phys. Chem. A, Vol. 107, No. 50, 2003 **10975**

frequencies calculated at the three DFT levels, it seems to be logical to assign this to 5^1, in agreement with the assignment by Kimura and co-workers. Even though $6b^1\beta CN^1$ may be an alternative based on the frequency alone, the very small Franck–Condon factor calculated for the latter, 0.001, is incompatible with the observation.

V. Summary and Conclusion

For a molecule with a large number of vibrational degrees of freedom such as $C_6H_5C{\equiv}CH^+$ and $C_6H_5C{\equiv}N^+$, assigning its vibrational spectrum can be a formidable job, especially when no additional information is available in the literature. In the case of two-photon ZEKE/MATI, further information can often be obtained through intermediate state selection. This is not the case in the one-photon scheme, even though the fact that excitation via an intermediate is not needed is its clear advantage in experimental terms. In our previous one-photon MATI investigation of $C_2H_3Br^+$,[22] it was demonstrated that use of the selection rule and calculated frequencies and Franck–Condon factors, especially those at the DFT levels, led to nearly complete assignment for its vibrational spectrum. The same strategy has been used with a striking success for the vibrational assignments for the cations of phenylacetylene and benzonitrile, which are much larger than $C_2H_3Br^+$. It is to be emphasized that the frequencies obtained at the DFT levels, especially BP86, provided nearly quantitative fit to the experimental data even though harmonic approximations were adopted for all of the vibrations. Cancellation of various errors must have acted favorably to result in such good fits. It is to be mentioned, however, that agreement between the calculated and measured frequencies is not sufficient for making a definite assignment. Comparing calculated and measured intensities would be helpful in this regard.

References and Notes

(1) Glassman, I. *Combustion*; Academic Press: San Diego, CA, 1996.

(2) Brasseur, G. P.; Orlando, J. J.; Tyndall, G. S. *Atmospheric Chemistry and Global Change*; Oxford University Press: New York, 1999.

(3) Cowley, C. R. *An Introduction to Cosmochemistry*; Cambridge University Press: Cambridge, U.K., 1995.

(4) Kimura, K.; Katsumata, S.; Achiba, Y.; Yamazaki, T.; Iwata, S. *Handbook of HeI Photoelectron Spectra of Fundamental Organic Molecules*; Japan Scientific Societies Press: Tokyo, 1981.

(5) Miller, T. A.; Bondybey, V. E. *Molecular Ions: Spectroscopy, Structure, and Chemistry*; North-Holland Publishing Company: New York, 1983.

(6) Baltzer, P.; Karlsson, L.; Wannberg, B.; Öhrwall, G.; Holland, D. M. P.; MacDonald, M. A.; Hayes, M. A.; von Niessen, W. *Chem. Phys.* **1997**, *224*, 95.

(7) Maier, J. P. In *Kinetics of Ion–Molecule Reactions*; Ausloos, P., Eds.; Plenum Press: New York, 1979.

(8) Müller-Dethlefs, K.; Sander, M.; Schlag, E. W. *Chem. Phys. Lett.* **1984**, *112*, 291.

(9) Hepburn, J. W. *Chem. Soc. Rev.* **1996**, *25*, 281.

(10) Schlag, E. W. *ZEKE Spectroscopy*; Cambridge University Press: Cambridge, U.K., 1998.

(11) Zhu, L.; Johnson, P. M. *J. Chem. Phys.* **1991**, *94*, 5769.

(12) Krause, H.; Neusser, H. J. *J. Chem. Phys.* **1992**, *97*, 5923.

(13) Park, S. T.; Kim, S. K.; Kim, M. S. *J. Chem. Phys.* **2001**, *114*, 5568.

(14) Park, S. T.; Kim, S. K.; Kim, M. S. *Nature* **2002**, *415*, 306.

(15) Park, S. T.; Kim, M. S. *J. Am. Chem. Soc.* **2002**, *124*, 7614.

(16) Ng, C. Y. *Annu. Rev. Phys. Chem.* **2002**, *53*, 101.

(17) Seiler, R.; Hollenstein, U.; Softley, T. P.; Merkt, F. *J. Chem. Phys.* **2003**, *118*, 10024.

(18) Kwon, C. H.; Kim, H. L.; Kim, M. S. *J. Chem. Phys.* **2002**, *116*, 10361.

(19) Kwon, C. H.; Kim, H. L.; Kim, M. S. *J. Chem. Phys.* **2003**, *118*, 6327.

(20) Kwon, C. H.; Kim, H. L.; Kim, M. S. *J. Chem. Phys.* **2003**, *119*, 215.

(21) Kwon, C. H.; Kim, H. L.; Kim, M. S. *J. Chem. Phys.* **2003**, *119*, 4305.

(22) Lee, M.; Kim, M. S. *J. Chem. Phys.* **2003**, *119*, 5085.

(23) Lee, M.; Kim, M. S. *J. Chem. Phys.*, in press.

(24) Becker, U.; Shirley, D. A. *VUV and soft X-ray photoionization*; Plenum Press: New York, 1996.

(25) Samson, J. A. R. *Techniques of Vacuum Ultraviolet Spectroscopy*; Wiley: New York, 1967.

(26) Frisch, M. J.; Trucks, G. W.; Schlegel, H. B.; Scuseria, G. E.; Robb, M. A.; Cheeseman, J. R.; Zakrzewski, V. G.; Montgomery, J. A., Jr.; Stratmann, R. E.; Burant, J. C.; Dapprich, S.; Millam, J. M.; Daniels, A. D.; Kudin, K. N.; Strain, M. C.; Farkas, O.; Tomasi, J.; Barone, V.; Cossi, M.; Cammi, R.; Mennucci, B.; Pomelli, C.; Adamo, C.; Clifford, S.; Ochterski, J.; Petersson, G. A.; Ayala, P. Y.; Cui, Q.; Morokuma, K.; Malick, D. K.; Rabuck, A. D.; Raghavachari, K.; Foresman, J. B.; Cioslowski, J.; Ortiz, J. V.; Stefanov, B. B.; Liu, G.; Liashenko, A.; Piskorz, P.; Komaromi, I.; Gomperts, R.; Martin, R. L.; Fox, D. J.; Keith, T.; Al-Laham, M. A.; Peng, C. Y.; Nanayakkara, A.; Gonzalez, C.; Challacombe, M.; Gill, P. M. W.; Johnson, B. G.; Chen, W.; Wong, M. W.; Andres, J. L.; Head-Gordon, M.; Replogle, E. S.; Pople, J. A. *Gaussian 98*, revision A.6; Gaussian, Inc.: Pittsburgh, PA, 1998.

(27) Duschinsky, F. *Acta Physicochim. URSS* **1937**, *7*, 551.

(28) Sharp, T. E.; Rosenstock, H. M. *J. Chem. Phys.* **1963**, *41*, 3453.

(29) Dyke, J. M.; Ozeki, H.; Takahashi, M.; Cockett, M. C. R.; Kimura, K. *J. Chem. Phys.* **1992**, *97*, 8926.

(30) Lichtenberger, D. L.; Renshaw, S. K.; Bullock, R. M. *J. Am. Chem. Soc.* **1993**, *115*, 3276.

(31) Araki, M.; Sato, S.; Kimura, K. *J. Phys. Chem.* **1996**, *100*, 10542.

(32) Watanabe, K.; Nakayama, T.; Mottl, J. *J. Quantum Spectrosc. Radiat. Transfer* **1962**, *2*, 369.

(33) Varsanyi, G. *Assignments for vibrational spectra of seven hundred benzene derivatives*; Adams Higer: London, 1974.

(34) Wilson, E. B., Jr. *Phys. Rev.* **1934**, *41*, 706.

(35) Neugebauer, J.; Hess, B. A. *J. Chem. Phys.* **2003**, *118*, 7215.